On the Display of the Atmospheric Circulation with Streamfunctions

MICHAEL HANTEL

Meteorologisches Institut der Universität Bonn, 53 Bonn, Federal Republic of Germany

(Manuscript received 22 March 1974, in revised form 21 June 1974)

ABSTRACT

The zonally averaged conservation equations for water, linear zonal momentum, and potential heat ($gz+c_pT$) are written in a form analogous to the mass continuity equation. This is possible when atmospheric storage terms are negligible which is generally the case during the solstice seasons. It follows that the fluxes of these properties can be represented by Stokes streamfunctions. Patterns of streamfunctions in the vertical-meridional plane for mass, water (all 3 phases combined), momentum, and heat have been prepared from the "Atmospheric Circulation Statistics" of Oort and Rasmusson (1971). They are shown for the seasons December–January–February and June–July–August, and for the area between 10S-75N. The following details are of interest:

1) The presented data are not new in any sense. Only the mode of presentation is new.
2) Contrary to the total mass transport, which is almost entirely conservative, all other transports have sources and sinks. They are treated as vertical flux divergences and thus are amenable to the streamfunction concept.
3) The streamfunction pattern can be considerably modified by linear combination with the mass continuity equation, characterized by a scale function: This function is zero for water transport, $a^2\Omega\cos^2\phi$ for momentum transport, and $gz_0+c_pT_0$ for heat transport (z_0, T_0 averages over total atmosphere). This choice minimizes the back-and-forth transport of properties by the cell circulation.
4) Boundary conditions are that the upper surface of the atmosphere be a streamline for mass, water, and momentum transport. For potential heat, the value at the upper surface at a certain latitude is the net radiation flux across this surface, integrated between this latitude and the pole.
5) The streamlines represent the total flux of the respective property in whatever form. For instance, vertical fluxes of water comprise mean and eddy components of all scales as well as net contributions of solid and liquid water flux.
6) The streamlines of transports with sources and sinks begin and end at the earth's surface (water, momentum, and heat) or additionally at the upper surface of the atmosphere (heat). There are no closed isolines.

The mixed character of the various fluxes is qualitatively described. Fluxes of different properties cross each other or go in opposite directions. Further, fluxes of the same property on different scales may go in opposite directions, particularly in the vertical. The total horizontal flux divergences are compared with some independent flux estimates at the earth's surface. Although there are still significant imbalances, the general agreement is fair.

1. Introduction

The zonally averaged continuity equation for the globe, if written in pressure coordinates, reads in conventional form

$$\frac{1}{\cos\phi}\frac{\partial[v]\cos\phi}{\partial y}+\frac{\partial[\omega]}{\partial p}=0. \tag{1.1}$$

The letters ϕ, y, p, v, ω designate, respectively, latitude, meridional coordinate ($y=a\phi$ with a=earth's radius), pressure, meridional wind component, and vertical wind component $\equiv dp/dt$. Brackets denote the zonal averaging operator. It has long been recognized that the physical content of this equation can be represented with a Stokes streamfunction Ψ defined by

$$[v]\equiv\frac{g}{2\pi a\cos\phi}\frac{\partial\Psi}{\partial p};\quad [\omega]\equiv-\frac{g}{2\pi a\cos\phi}\frac{\partial\Psi}{\partial y}, \tag{1.2}$$

where g represents gravity. Hemispheric and global patterns of Ψ have been discussed by many authors. The early attempts to display the global Ψ-distribution were hampered by the inaccuracy of the available $[v]$-values (Mintz and Lang, 1955). Northern Hemisphere patterns of Ψ in its annual course, based on the most recent measurements, have been presented by Oort and Rasmusson (1970). Figs. 1 and 2 show for reference the mass transport streamfunction Ψ for winter and summer,[1] recalculated from the seasonal values of the balanced meridional wind (Oort and Rasmusson, 1971).

A critical comparison of these data with earlier compilations, notably those of Palmén and Vuorela (1963) for the winter season (December–January–February) and of Vuorela and Tuominen (1964) for the

[1] In this paper all seasons refer to Northern Hemisphere.

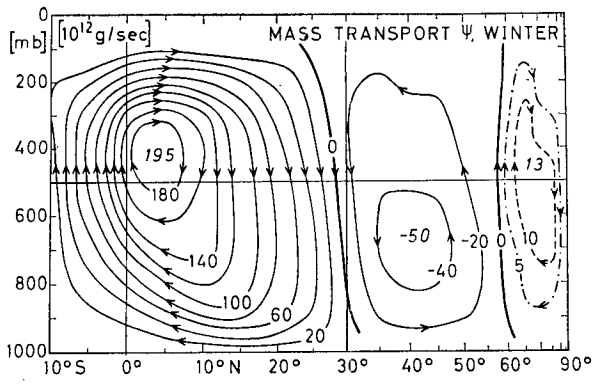

FIG. 1. Streamfunction for atmospheric mass transport in units 10^{12} gm sec^{-1} for season December–January–February. Data from Oort and Rasmusson (1971).

summer season (June–July–August) has been given by Oort and Rasmusson (1970). The patterns of the latter, as redrawn in our Figs. 1 and 2, compare favorably with other calculations by Newell *et al.* (1972), at least for winter. In summer, our Fig. 2 shows a weak and broadly distributed Ferrel cell and an almost nonexisting northern Hadley cell, whereas Newell *et al.* report a well-defined Ferrel cell between 33N and 70N and likewise a well-defined northern Hadley cell throughout the troposphere between 16N–33N.

It is well known that the weakness and variability of the Ferrel cell stems from the fact that this indirect circulation is the result of mass fluxes of considerable strength but opposite direction (Oort and Rasmusson, 1970, Fig. 11). Consequently, one should not put too much emphasis on the exact figure of the small residual Ferrel cell. This argument applies particularly to annual patterns of the mass streamfunction. As has been pointed out by Lorenz (1969) and can be seen by inspection of Figs. 1 and 2 in Oort and Rasmusson's paper, even the tropical Hadley cells become relatively weak in the annual average and sensitive to slight changes in the underlying data. Obviously, this is due to the seasonal migration of the rising branches of the Hadley cell of either hemisphere.

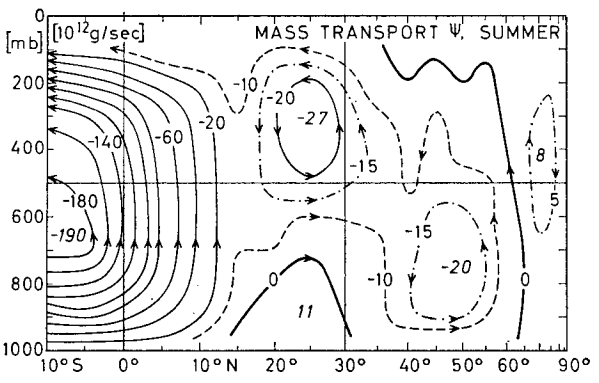

FIG. 2. Like Fig. 1 but for season June–July–August.

Several investigators have tried to overcome the uncertainty in the $[v]$-data required to calculate Ψ by employing other conservation equations. Mintz and Lang (1955) derived the meridional mass circulation over the Northern Hemisphere from the angular momentum equation. Due to certain inherent assumptions, for example that the vertical eddy momentum flux vanishes above 700 mb, they found only $80–90\times10^{12}$ gm sec^{-1} for the winter Hadley cell. Newton (1972) also applied the concept of angular momentum balance for estimating the meridional mass circulation as a residual. In Northern Hemisphere summer (Newton's Fig. 9.12) he found 4 cells between equator and 30N with a net upward transport of the order of 50×10^{12} gm sec^{-1} between 20N and 30N, whereas our Fig. 2 reveals no sizeable upward or downward transport in this region. Further, in Southern Hemisphere summer, Newton found the rising branch of the southern Hadley cell to transport approximately 100×10^{12} gm sec^{-1} between 10S and the equator, whereas our Fig. 1 shows an upward transport of nearly double strength in this region.

These comments about the reliability of the existing estimates of the mean meridional circulation might suffice. It is not intended in this study to give a comparison in any complete sense of the various balance calculations carried out in the past, although we shall provide some critical remarks. We rather maintain that the representation in terms of a streamfunction gives a simple and complete account of both the vertical and meridional flux of a physical quantity.

The mass transport is not the only quantity that can be portrayed in this form. Palmén and Newton (1969) plotted the streamfunction of the total water vapor flux (see next section). Likewise, they plotted as quasi-streamfunction the meridional geostrophic eddy flux of sensible heat (winter of 1949). Lorenz (1951) discussed the winter streamfunction pattern of relative angular momentum based on geostrophic data. Newell *et al.* (1972), according to formulas discussed in Starr *et al.* (1970), plotted the streamfunction for the total angular momentum transport, based on the most recent and complete data. It will be shown in Section 3 that their approach tends to obscure the relevant momentum transport due to the overwhelmingly large back-and-forth transport of earth angular momentum. Concerning the atmospheric heat transport, no attempt seems to have been made yet to portray it in flux form. We shall show that, with a proper choice of the boundary condition for the pressure surface zero, it is possible to define in a non-arbitrary way a streamfunction for the potential heat transport.

It is the aim of this paper to bring the conservation equations of all relevant meteorological field quantities into a form comparable to Eq. (1.1). The zonally averaged patterns of these quantities like wind, temperature, geopotential, and humidity are maintained by a variety of horizontal and vertical transport

mechanisms. It is obvious from the outset that both mean and eddy contributions will enter the streamfunctions for the respective quantities. The usefulness of such a mixed representation is that the overall transport becomes visible. This will allow intercomparisons between the transport mechanisms for the different field quantities.

Before considering the streamfunctions in detail we shall note an obvious generalization of Eqs. (1.1), (1.2). Let us assume that the meridional and vertical fluxes F_y, F_p of a certain property obey the generalized transport equation

$$\frac{1}{h_y}\frac{\partial(h_y F_y)}{\partial y}+\frac{1}{h_p}\frac{\partial(h_p F_p)}{\partial p}=0, \tag{1.3}$$

with dimensionless functions $h_y\equiv h_y(y)$, $h_p\equiv h_p(p)$. This equation can be satisfied by a streamfunction Ψ_F:

$$F_y\equiv\frac{g}{2\pi a}\frac{1}{h_y h_p}\frac{\partial\Psi_F}{\partial p},\quad F_p\equiv-\frac{g}{2\pi a}\frac{1}{h_y h_p}\frac{\partial\Psi_F}{\partial y}. \tag{1.4}$$

It is important that the function h_y depends on y only, h_p on p only. In most, but not all, cases we shall choose $h_y=\cos\phi$, $h_p\equiv 1$.

Three points are important when applying Eq. (1.3) to transports of atmospheric quantities. The first is that the respective pattern must be stationary. Otherwise (1.3) does not hold. Thus we can strictly apply Eq. (1.3) only during extreme seasons. Even then, as has been shown by Newton (1972), there can be sizeable storage or "spinup-spindown" terms in the conservation equations. In this study, we shall restrict ourselves to the extreme seasons. All storage terms, if they appear, are small and formally included in the vertical transport flux divergence.

The second point is the treatment of the source terms. Source terms are, for example, the rate of condensation or sublimation in the water transport equation, or the diabatic radiational heating in the first law of thermodynamics. We consider here all transportable quantities as conservative. This means, according to Van Mieghem (1973), that the source terms can be represented by the divergence of a properly chosen vector field. Moreover, we shall consider only the vertical flux component of the respective source vectors. This will be discussed for the different transports in the subsequent sections.

The third point is concerned with the boundary conditions. Atmospheric streamfunctions, except for the mass transport, generally have the constraint that streamlines begin and end at the earth's surface, due to the exchange between earth and atmosphere. The energy streamlines also cross the upper surface of the atmosphere as a consequence of the radiational exchange with space. We shall specify the boundary conditions for the streamfunctions at the upper surface of the atmosphere.

All data evaluations of the present study are based on the "Atmospheric Circulation Statistics" of Oort and Rasmusson (1971). This data collection covering the period May 1958 through April 1963 provides monthly, seasonal, and yearly averages of zonally and time-averaged field quantities, and standing and transient eddies (except transient eddy fluxes in the vertical direction). The data are on the standard levels 1000, 950, 900, 850, 700, 500, 400, 300, 200, 100 and 50 mb between 10S–75N, with a meridional resolution of 5°. We consider this basic data set the best available prerequisite for consistent results.

2. The water transport streamfunction

The water transport equation in the zonally and time-averaged form reads

$$\frac{1}{\cos\phi}\frac{\partial[\overline{vq}]\cos\phi}{\partial y}+\frac{\partial[\overline{\omega q}]}{\partial p}=[\overline{Q_q}], \tag{2.1}$$

where q is the specific humidity, and the overbar denotes the time-average. The source function for water may be written:

$$Q_q\equiv g\frac{\partial}{\partial p}(H_C+H_q). \tag{2.2}$$

In (2.2), H_C is the vertical flux of condensed water, either in fluid or frozen form; H_q denotes the vertical flux of water vapor due to microscale turbulent diffusion (molecular diffusion included). Both fluxes H have the physical dimension kg m^{-2} sec^{-1} and are positive upward. No horizontal components of these fluxes are taken into account because we consider them to be of negligible importance on this scale.

Following Palmén and Newton (1969, Fig. 17.6) we introduce a modified vertical flux F_q of water substance defined by

$$F_q\equiv\omega q-gH_C-gH_q. \tag{2.3}$$

Eq. (2.1) is identically satisfied if we define a streamfunction Ψ_q by

$$[\overline{vq}]\equiv\frac{g}{2\pi a\cos\phi}\frac{\partial\Psi_q}{\partial p},\quad[\overline{F_q}]\equiv-\frac{g}{2\pi a\cos\phi}\frac{\partial\Psi_q}{\partial y}. \tag{2.4}$$

Figs. 3 and 4 show the pattern of the water transport function for winter and summer. Typical values of Ψ_q are in the range 10^{11}–10^{12} (gm water) sec^{-1}. This might be compared with values of the mass transport streamfunction of the order of 10^{14} (gm air) sec^{-1}.

The basic difference between the two streamfunctions Ψ and Ψ_q is the property of the latter, to have built-in sources: the streamlines of Ψ_q begin and end at the earth's surface (the boundary condition in Figs. 3 and 4 is $\Psi_q\equiv 0$ at the upper surface of the atmosphere). The physical meaning of the vertical gradient of Ψ_q is the

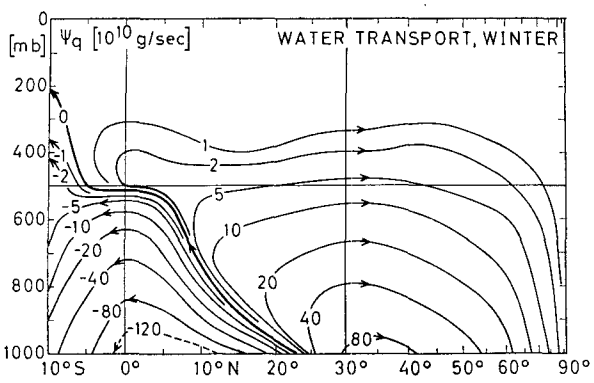

FIG. 3. Streamfunction for atmospheric water transport in units 10^{10} gm sec^{-1} for December–January–February. Data from Oort and Rasmusson (1971). Note quasi-logarithmic scale of isolines. Horizontal transports: water vapor only. Vertical transports: vaporous, liquid, and frozen water.

horizontal transport of water *vapor;* no horizontal transport of condensed water is assumed to take place. The horizontal gradient of Ψ_q, however, determines the vertical flux of water *substance*, in gaseous, fluid, or solid form. In other words, Ψ_q comprises different physical processes in a mixed manner.

We turn now to another aspect of the water transport streamfunction and make some speculative remarks about the fluxes H_C and H_q. Not very much is known about the vertical profiles of these quantities. It seems certain, however, that H_C (which gives by definition the vertical flux of condensed water substance) is negative (downward) everywhere in the vertical, at least when time- and space-averaged. Concerning H_q, no profile measurements are available. Several authors (Holland and Rasmusson, 1973; Augstein *et al.*, 1973; Nitta and Esbensen, 1974) incorporate H_q into the correlation part of $[\overline{\omega q}]$, considering it as subgrid-scale. For the present discussion, we maintain that the subgrid-scale transport comprises at least two different mechanisms: the *convective* scale subgrid transport, which is an organized transport properly described by the eddy concept, and the *microturbulent* transport H_q, which is due to three-dimensional turbulence approximately described by the diffusion concept. We hypothetically assume that these two can be objectively separated from each other.

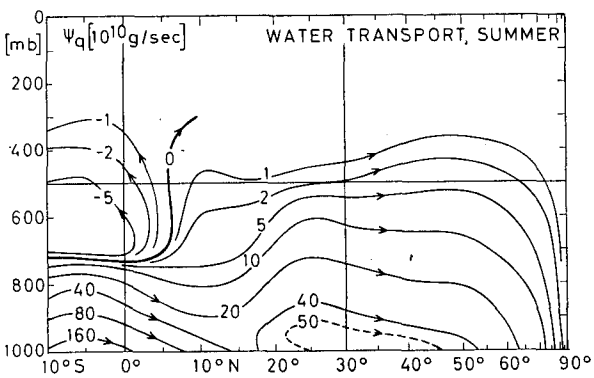

FIG. 4. Like Fig. 3 but for June–July–August.

Taking these viewpoints for granted, H_q should be positive everywhere in the vertical: the vertical diffusive water vapor flux should be directed down the gradient of specific humidity, i.e., upward. Furthermore, it seems reasonable to assume that H_C and H_q are, on the global scale, of similar orders of magnitude. Finally, in order to account for the evaporation of falling precipitation in the lowest layers close to the earth's surface, H_C should have an extremum in the middle or lower atmosphere.

Fig. 5 sketches the hypothetical vertical profiles of these functions. There exists in the lower part of the troposphere a water vapor source (positive p-gradient of H_C+H_q between surface and height of the minimum) and a sink above that level. Thus the vertical transport of water must diverge in the lower and converge in the upper troposphere. Recent evaluations of the BOMEX data for the Atlantic trades between 500–1000 mb support this conclusion: Nitta and Esbensen (1974) report a strong moisture source in this layer both for undisturbed and disturbed conditions. It is obvious from Fig. 5 that the surface values of $[\overline{H_C}]$ and $[\overline{H_q}]$ are equal to the zonally and time-averaged surface precipitation and evaporation, respectively. Since there exist estimates of both these surface quantities, speculation concerning H_C and H_q is restricted to the specific vertical patterns.

Turning now back to expression (2.3) for F_q, taking time and longitudinal averages ($X=\bar{X}+X'$ for time-dependence and $X=[X]+X^*$ for longitude-dependence) we find that

$$[\overline{F_q}]=[\bar{\omega}][\bar{q}]+[\bar{\omega}^*\bar{q}^*]+[\overline{\omega'q'}]-g[\overline{H_C}]-g[\overline{H_q}]. \quad (2.5)$$

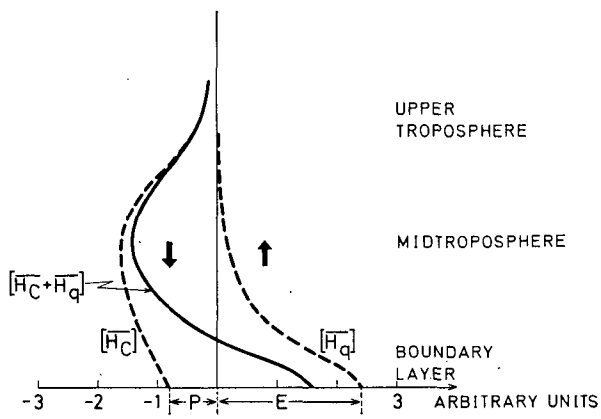

FIG. 5. Speculative vertical profiles of zonally averaged vertical precipitation flux $[\overline{H_C}]$ and vertical diffusive water vapor flux $[\overline{H_q}]$. Divergence of sum of both is source term in water transport equation. Surface values of $[\overline{H_C}]$, $[\overline{H_q}]$ are negative precipitation $-P$ and evaporation E, respectively.

The first three terms on the righthand side are denoted, following common usage, the mean water vapor transport due to meridional circulation, to standing eddies, and to transient eddies, respectively. The mean and standing transports can be considered to be known (Oort and Rasmusson, 1971), as well as can the diffusive flux using a standard parameterization

$$[\overline{H_q}] \equiv \rho A_q g \frac{\partial [\bar{q}]}{\partial p}. \tag{2.6}$$

In (2.6), A_q is some turbulent exchange coefficient, supposed to be a smooth function of latitude and height. Formula (2.6) is applicable for mean conditions since $[\bar{q}]$ decreases uniformly with height. Further, the vertical gradient of $[\bar{q}]$ has in all latitudes its maximum value at the sea surface.

We then see that (2.5), together with (2.6), allows one to determine the sum

$$[\overline{\omega' q'}] - g[\overline{H_C}] \tag{2.7}$$

as a residual function. It is not surprising that the vertical transport $[\overline{\omega' q'}]$ due to transient eddies cannot be inferred from daily radiosonde measurements. Sizeable contributions to this term are to be expected in the interior of mesoscale towering cumulonimbus clouds, particularly in the tropics (Riehl and Malkus, 1958). This hot-tower process transports transient deviations from the average of conservative properties upward; downward processes happen on a considerably larger scale, but with very low vertical velocities, in the cloud-free regions. It would be of great interest to further separate the quantity $[\overline{\omega' q'}]$ into a synoptic-scale and a subgrid-scale contribution. The latter part would presumably be due to the hot-tower process and would intimately be related to H_C. The former could be gained from daily observations provided these would yield reliable synoptic-scale vertical velocity patterns.

The winter transport pattern in Fig. 3 compares favorably with Fig. 17.6 in Palmén and Newton (total flux of water vapor in Northern Hemisphere, six cooler months of 1958). The transport lines leaving the earth's surface indicate excess of evaporation over precipitation, whereas lines entering the surface show a zonal mean surplus of precipitation. In winter, a net total of more than 200×10^{10} gm sec^{-1} of water leaves the surface between 5N and 35N. The smaller part of this flux (80 units) is transported via eddy exchange mechanisms across 30N into middle and higher latitudes. The greater part (120 units) is transported across the equator, mostly into the Southern Hemisphere tropics, the rest into the higher latitudes of the Southern Hemisphere. The area 5N-10S with the highest precipitation excess coincides with the latitudinal precipitation maximum as reported by Möller (1951).

In summer, the tropical transport pattern is reversed. A little over 160 units enter the Northern Hemisphere across the equator. Most of it ($\simeq$120) precipitates in the belt equator-15N (the ITCZ-region). The remaining 40 units, together with a contribution of 10 in the trades region 17N-30N, enter the middle and higher latitudes. The midlatitude surplus of precipitation over evaporation beyond 50N is not too variable during the course of the year.

Comparison of the horizontal water flux divergence with the vertical flux components at the earth's surface is standard in studies concerning the atmospheric water transport, for instance: Palmén and Vuorela (1963), and Vuorela and Tuominen (1964) for the extreme seasons; Starr *et al.* (1969), for the IGY (1958) annual mean; or Rasmusson (1972) for the area covered in the present study with main emphasis on the tropics. Rasmusson's evaluation is based on much the same data as is the present study. In particular, Rasmusson was forced to obtain the monthly precipitation values as residual terms in the balance equation.

Since the investigations just mentioned provide a wealth of information concerning the characteristics of atmospheric water transport, it is not necessary to repeat the balance considerations in detail. We refer particularly to the work of Rasmusson for his extensive presentation and critical discussion of the balancing terms.

In order to account for the magnitude of the error in the different quantities, we consider only briefly the vertically integrated balance equation

$$\frac{1}{2\pi a \cos\phi} \frac{\partial \Psi_{q,s}}{\partial y} = E - P. \tag{2.8}$$

Here, $\Psi_{q,s}$ is the value of the streamfunction at the earth's surface, E is evaporation, P precipitation. Storage terms are neglected in (2.8), as are any possible contributions of the term $[\overline{\omega q}]$ at the sea surface due to non-coincidence of pressure and geopotential surfaces or to pressure tendencies. Both sides of equation (2.8) are compared in Fig. 6 in the same physical units. The E-P curves are taken from Newell *et al.* (1969) which are only partly based on atmospheric flux measurements. For winter, Schutz and Gates (1971) provide seasonal precipitation values, determined from a Russian source, and January evaporation values, determined from Budyko (1963). Though the broad pattern is in agreement, some systematic differences are intriguing, notably between 5S–10N and 70N–75N in winter. It is not clear which quantity is responsible for the errors. The author feels, however, that the precipitation values are to be considered with caution. Referring forward to Fig. 11, the comparison of precipitation estimates reveals appreciable differences between Schutz and Gates and the earlier results of Möller (1951). Due to its mesoscale and patchy nature, particularly in the tropics, precipitation can hardly be determined by the present observation net with the

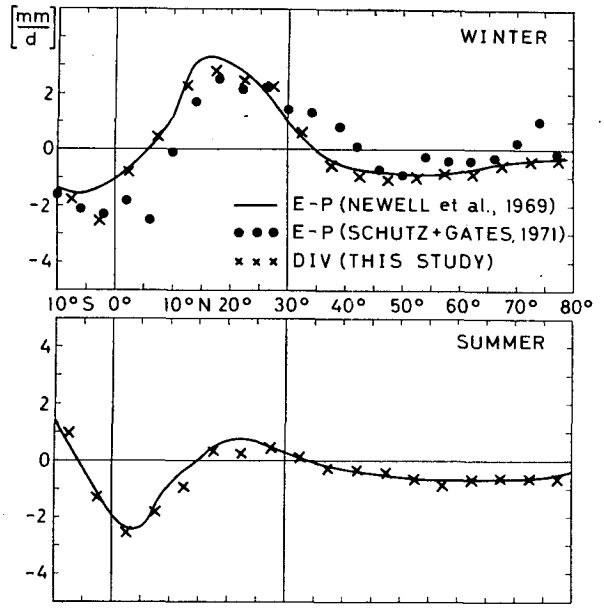

FIG. 6. Zonally averaged atmospheric water balance in mm day^{-1} for solstice seasons. Full curves: surface evaporation (E) minus precipitation (P) according to Newell *et al.* (1969), partly based on atmospheric data. Dots: E-P according to Schutz and Gates (1971), based on surface data (winter only). Crosses: divergence of water vapor streamfunction at earth's surface, calculated from Figs. 3 and 4.

necessary accuracy. Keeping this fact in mind, the agreement of the independently determined data of Schutz and Gates for E-P and of this study for the atmospheric divergence must be considered fair.

3. The momentum transport streamfunction

The absolute angular momentum per unit area of an air parcel moving at latitude ϕ with eastward velocity component u is

$$I = a\cos\phi(u + a\Omega\cos\phi). \tag{3.1}$$

We neglect the height dependence of angular momentum (see Newton, 1972) because it is of minor importance for the subsequent discussion. We note in passing that, if height dependence is being incorporated in (3.1), another effect would also have to be taken into account: the ellipticity of the earth. This effect, seemingly not discussed yet, should be of similar magnitude as is the height dependence of I because the deviation of the earth from ideal sphericity is of the order of the scale height of the atmosphere. The total time derivative of I is

$$\frac{dI}{dt} = a\cos\phi\left(\frac{du}{dt} - fv - \frac{uv}{a}\tan\phi\right), \tag{3.2}$$

where $f = 2\Omega\sin\phi$ denotes the Coriolis parameter. The expression in brackets can be eliminated by means of the x-equation of motion in pressure coordinates, which yields

$$\frac{dI}{dt} = -a\cos\phi\left(\frac{\partial\Phi}{\partial x} + g\frac{\partial\tau_x}{\partial p}\right). \tag{3.3}$$

Here, Φ is the geopotential and τ_x the x-component of horizontal stress. No horizontal stress variations are taken into account. Expanding the total time derivative into flux form and averaging with respect to longitude and time we find

$$\frac{1}{\cos\phi}\frac{\partial[\overline{vI}]\cos\phi}{\partial y} + \frac{\partial}{\partial p}\{[\overline{\omega I}] + ga\cos\phi[\overline{\tau_x}]\} = 0. \tag{3.4}$$

Mountain torques (White, 1949) are formally included by interpreting τ_x to contain both the zonal stress as well as the net geopotential difference in zonal direction across the mountain barriers of the respective latitude circle.

Eq. (3.4) has the desired form (1.1) of a continuity equation and it seems straightforward to construct a streamfunction for absolute angular momentum transport in direct analogy to (1.2); see Fig. 4.13 in Newell *et al.* (1972). This approach has the drawback that it reproduces to a large extent the mean meridional (toroidal) circulation times the factor $\cos^2\phi$. This is due to the obscuring back-and-forth transport of earth angular momentum. This point has already been discussed by Lorenz (1951) who plotted streamlines of angular momentum for the period 1 November 1945 through February 1946. Lorenz noted that a rather weak meridional cell could transport large amounts of Ω-angular momentum whence he made sure that any flow of angular momentum due to mean meridional circulations had been omitted. Smagorinsky (1963) also used the streamfunction display for the zonal momentum flux resulting from a numerical experiment.

Following Lorenz's argument we consider the meridional flux of total angular momentum:

$$[\overline{vI}] = a\cos\phi\{[\overline{vu}] + [\bar{v}]a\Omega\cos\phi\}. \tag{3.5}$$

The second righthand-side term (Ω-momentum transport) is more than an order of magnitude layer than the first (u-momentum transport), irrespective of the fact that only the u-momentum transport contains relevant meteorological information. The same is true of the vertical flux $[\overline{\omega I}]$. Thus we write Eq. (3.4) in the equivalent form

$$\frac{1}{\cos\phi}\frac{\partial}{\partial y}\{a\cos\phi[\overline{vu}]\}\cos\phi + \frac{\partial}{\partial p}\{a\cos\phi[\overline{\omega u}] + ga\cos\phi[\overline{\tau_x}]\} + D = 0. \tag{3.6}$$

Here, D is that part of the divergence of total angular

momentum flux that is solely due to the earth's rotation:

$$D\equiv\frac{1}{\cos\phi}\frac{\partial}{\partial y}\{a^2\Omega\cos^2\phi[\bar{v}]\}\cos\phi+\frac{\partial}{\partial p}\{a^2\Omega\cos^2\phi[\bar{\omega}]\}. \quad (3.7)$$

By eliminating the mass flux divergence from D with the aid of Eq. (1.1) we find

$$D=-a\cos\phi f[\bar{v}]. \quad (3.8)$$

Thus the influence of the earth's rotation on the momentum balance reduces to the familiar Coriolis term which depends on the mean meridional wind. Consequently, we introduce for $[\bar{v}]$ the mass transport streamfunction Ψ. It is possible then to combine all derivatives with respect to p into a single expression that transforms Eq. (3.6) into

$$\frac{1}{\cos\phi}\frac{\partial}{\partial y}\{a\cos\phi[\overline{vu}]\}\cos\phi+\frac{\partial}{\partial p}\left\{a\cos\phi([\overline{\omega u}]+g[\overline{\tau_x}])-\frac{fg}{2\pi}\Psi\right\}=0. \quad (3.9)$$

We first note that this equation for relative angular momentum can be visualized as a "linear" combination of the equations for total angular momentum and mass continuity, symbolically: Eq. (3.9) = Eq. (3.4) minus [Eq. (1.1) times the scale function $a^2\Omega\cos^2\phi$]. This will remove all closed streamlines that are present in the absolute angular momentum streamfunctions of Newell *et al.* (1972). Further, in the horizontal transport component there is no contribution of the earth's rotation anymore; its influence is condensed in the Coriolis term, which is considerably smaller than the Ω-momentum terms in (3.4). If we adopt the conservative estimates

$$\left.\begin{array}{ll} u\simeq 10\text{ m sec}^{-1} & \Psi\simeq 5\times10^{10}\text{ kg sec}^{-1} \\ \omega\simeq 10^{-3}\text{ mb sec}^{-1} & \phi\simeq 43^\circ \\ \tau_x\simeq 1\text{ dyne cm}^{-2} & \end{array}\right\}, \quad (3.10)$$

all terms in the vertical momentum transport component have comparable orders of magnitude.

Eq. (3.9) expresses conservation of *angular momentum*. If we regard (3.9) as the maintenance equation for the zonal wind it seems meteorologically more natural to look at it from the *linear momentum* viewpoint. Dividing by $a\cos\phi$ we obtain

$$\frac{1}{\cos^2\phi}\frac{\partial}{\partial y}[\overline{vu}]\cos^2\phi+\frac{\partial[\overline{F_u}]}{\partial p}=0, \quad (3.11)$$

with the generalized vertical momentum flux

$$F_u\equiv\omega u+g\tau_x-f\frac{g}{2\pi a\cos\phi}\Psi. \quad (3.12)$$

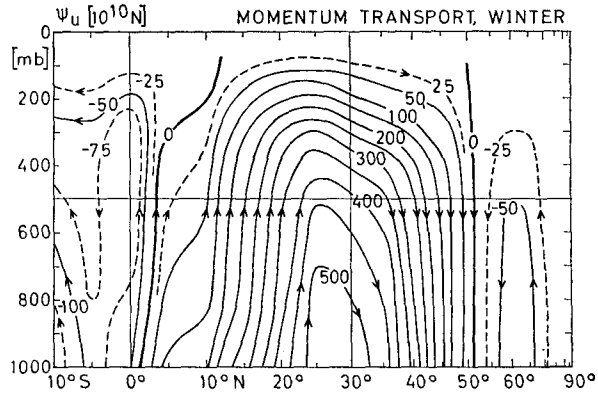

FIG. 7. Streamfunction for atmospheric linear momentum transport in units 10^{10} newtons (N) for December–January–February. Data from Oort and Rasmusson (1971). To compare with Hadley units (1 HU $\equiv 10^{18}$ J) note that 10^{10} N corresponds to 6.37×10^{-2} HU.

Eq. (3.11) is virtually identical with the time-averaged zonal-index equation (5a) of Mintz (1955) or with the zonal wind equation (4.16) of Newell *et al.* (1972); however, these authors did not further follow the lines as studied here. According to (3.11), (3.12), the impact of the mass transport streamfunction Ψ on the vertical transport of zonal wind is obvious (see also Newton, 1972). We now introduce the momentum transport streamfunction Ψ_u by

$$[\overline{vu}]\equiv\frac{g}{2\pi a\cos^2\phi}\frac{\partial\Psi_u}{\partial p};\quad [\overline{F_u}]\equiv-\frac{g}{2\pi a\cos^2\phi}\frac{\partial\Psi_u}{\partial y}. \quad (3.13)$$

The physical unit of Ψ_u is 1 newton = 1 (kg m sec^{-1})sec^{-1}. Separating the unit this way illustrates that Ψ_u transports momentum (unit 1 kg m sec^{-1}) similarly to Ψ, with unit 1 kg sec^{-1}, which transports mass. Figs. 7 and 8 show patterns of the momentum streamfunction for winter and summer, calculated from the seasonal data of $[\overline{vu}]$ as listed in Oort and Rasmusson (1971). Ψ_u was determined by vertically integrating, downward, the lefthand equation of (3.13); the boundary condition at the upper surface of the atmosphere was $\Psi_u\equiv0$.

Fig. 7 corroborates the early results of Widger (1949) and notably Lorenz (1951), which have been presented in a similar format though based only on preliminary data (geostrophic winds, no data above 7.5 km height). Figs. 7 and 8 reproduce the general pattern of the global momentum transport: upward transport of westerly momentum in the tropics, poleward transport in the middle and upper troposphere, downward transport in middle latitudes. A distinct, though relatively weak, polar cell is apparent which reveals the highest latitudes between 65N–90N to be a momentum source throughout the year. The winter circulation is much stronger than the summer circulation. There is a net transport of momentum across the equator towards the

Summer Hemisphere: in Fig. 7 there flow 50 units southward, in Fig. 8 some 125 units northward. The net annual flux is northward, in accord with Henning's (1968) estimates. The downward transport of momentum in the inner tropics just north of the equator in summer is clearly associated with the zone of equatorial westerlies during this season, notably over the Indian Ocean longitudes (Flohn, 1949, 1953).

Comparison of the horizontal momentum flux divergence with the vertical flux at the earth's surface is standard in studies concerning the atmospheric momentum transport, notably Newton (1971). The surface vertical momentum transport comprises mainly frictional and mountain torque, the other contributions (spin-up, spin-down, the height effect together with the ellipticity effect, seasonal mass drift, and water momentum flux) being lumped together by Newton into "miscellaneous torques." During the solstice seasons, the miscellaneous torques are about an order of magnitude smaller than the other fluxes.

Table 1 compares different estimates of total horizontal fluxes across three latitude circles. The estimates of the present study are simply the surface streamfunction values of Figs. 7 and 8, respectively, multiplied by the earth's radius. In view of different assumptions and data sources used by various authors, the results compare favorably.

4. The streamfunction for potential heat

Whereas the streamfunction for mass transport is entirely free of arbitrary assumptions due to the fact that there are no sources or sinks of atmospheric air (except the small water flux effect, see next section, and except long-term climatic changes of total atmospheric mass), both the water and the momentum flux streamfunctions have sources and sinks that show up in very significant flux components across the earth's surface. In addition to these surface fluxes that are due to phase changes and nonlinear (frictional) effects, a continuous energy exchange with space takes place across the atmosphere's upper surface due to radiation fluxes. In

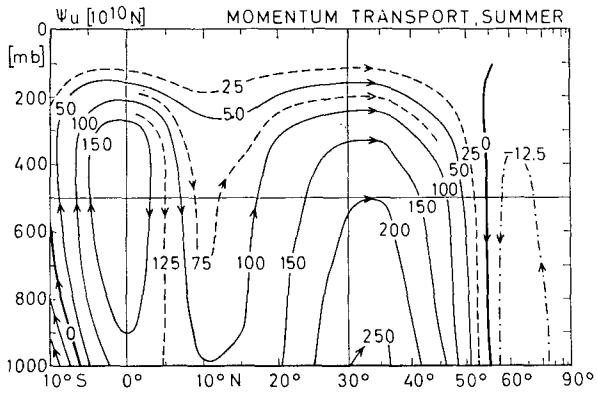

FIG. 8. Like Fig. 7 but for June–July–August.

TABLE 1. Total linear momentum flux across latitudes 0°, 30°, 60N, in Hadley units (1 HU = 10^{18} J), estimated by different authors. Values in this study calculated by vertical integration of Oort and Rasmusson's (1971) tables. To compare with momentum streamfunction note that 1 HU corresponds to 15.70×10^{10} N.

		0°	30°N	60°N
Dec–Jan–Feb	Newton (1971)	−4	42	−4
	Newell *et al.* (1972)	−6	43	−1
	This study (surface flux from Fig. 7)	−3.5	33.4	−4.4
Jun–Jul–Aug	Newton (1971)	13	14	−1
	Newell *et al.* (1972)	11	15	−1
	This study (surface flux from Fig. 8)	8.9	15.9	−1.6

the subsequent treatment we shall consider only the vertical component of the radiation flux.

The time- and zonally-averaged thermodynamic energy equation reads, in conventional notation,

$$\frac{1}{\cos\phi}\frac{\partial c_p[\overline{vT}]\cos\phi}{\partial y}+\frac{\partial c_p[\overline{\omega T}]}{\partial p}=\frac{R}{p}[\overline{\omega T}]+[\overline{Q_T}]. \quad (4.1)$$

Here, c_p is the specific heat for constant pressure; the diabatic heating function may be written:

$$Q_T\equiv g\frac{\partial}{\partial p}(H_R+H_T-LH_C); \quad (4.2)$$

H_R is the vertical flux of short- plus long-wave radiation and H_T is the vertical component of the diffusive temperature flux. Both H_R and H_T are positive upward and have physical dimensions $J\ m^{-2}\ sec^{-1}$; H_C is the vertical flux of condensed water substance as defined in Section 2, and L the latent heat of condensation. Concerning the mutual rôle of $[\overline{H_T}]$ and $c_p[\overline{\omega'T'}]$, compare the above discussion of H_q. Like H_q, H_T is considered to comprise only microturbulent (as well as molecular diffusive) fluxes of T.

In addition to the sensible heat equation (4.1) we consider the hydrostatic equation in the form

$$\frac{d\Phi}{dt}=-\frac{\omega}{\rho}. \quad (4.3)$$

Eq. (4.3) is valid for negligible pressure tendency (which is approximately the case in this study) and negligible horizontal pressure advection (which is usually 2 orders smaller than the vertical advection even in actual cases). Averaging of (4.3) with respect to time and longitude and adding it to (4.1) yields the conservation equation for the quantity $H\equiv c_pT+gz$:

$$\frac{1}{\cos\phi}\frac{\partial[\overline{vH}]\cos\phi}{\partial y}+\frac{\partial[\overline{\omega H}]}{\partial p}=[\overline{Q_T}]. \quad (4.4)$$

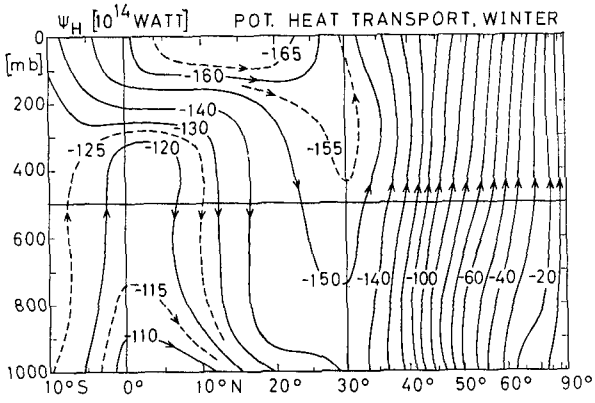

FIG. 9. Streamfunction for atmospheric potential heat transport in units 10^{14} J sec^{-1} for December–January–February. Data from Oort and Rasmusson (1971) for atmospheric transports and from Newell *et al.* (1969) for radiation balance of earth-atmosphere-system.

In (4.4), H has been synonymously called the Montgomery streamfunction, dry static energy, or potential heat. In the present study we shall prefer the latter name. It is the shortest and, more importantly, it is closely related to potential temperature. The horizontal transport components of c_pT and gz are to a considerable degree opposed to each other (Oort, 1971). The mean c_pT-transport is in all latitudes opposed to the mean gz-transport. The eddy gz-transport is negligible. The eddy c_pT-transport is large in midlatitudes but only 25% of either the mean c_pT- or gz-transport in the tropics (Oort and Rasmusson, 1970). The dominating effect of the mean circulation is easily seen by a glance at the vertical profile of the potential heat: H varies between 260 J gm^{-1} at the earth's surface and 360 J gm^{-1} in the stratosphere. Thus the relative differences of H are of the order of 30%, i.e., the mean meridional circulation causes, similarly to the angular momentum transport, a very large back-and-forth transport of energy that has no meteorological significance.

We thus introduce the average value of potential heat throughout the atmosphere

$$H_0 \equiv 317.4 \text{ J gm}^{-1}, \tag{4.5}$$

corresponding to a potential temperature of 317.4K. We multiply the mass continuity equation (1.1) with H_0 and subtract it from Eq. (4.4). With the generalized fluxes

$$F_{H,y} \equiv [\overline{Hv}] - H_0[\bar{v}];$$
$$F_{H,p} \equiv [\overline{H\omega}] - H_0[\bar{\omega}] - g[\overline{H_R} + \overline{H_T} - L\overline{H_C}] \tag{4.6}$$

we obtain the reduced conservation equation for potential heat,

$$\frac{1}{\cos\phi}\frac{\partial F_{H,y}\cos\phi}{\partial y} + \frac{\partial F_{H,p}}{\partial p} = 0. \tag{4.7}$$

Analogously to the interpretation of the relative angular momentum equation (3.9), we visualize Eq. (4.7) as a linear combination of Eq. (4.4) with the mass continuity equation (1.1) times the scale factor H_0. The introduction of a streamfunction Ψ_H into (4.7) is straightforward:

$$F_{H,y} \equiv \frac{g}{2\pi a\cos\phi}\frac{\partial \Psi_H}{\partial p}; \quad F_{H,p} \equiv -\frac{g}{2\pi a\cos\phi}\frac{\partial \Psi_H}{\partial y}. \tag{4.8}$$

The physical units of Ψ_H are 1 J sec^{-1} = 1 watt. The boundary condition for Ψ_H at the upper surface of the atmosphere can be constructed by the known flux $F_{H,p=0}$, which comprises only the radiative flux H_R since all other components are accompanied by material transports and vanish in the zero pressure level. We thus have

$$\Psi_{H,p=0}(y) = 2\pi a\int_{SP}^{y}\cos\phi[\overline{H_{R,p=0}}]dy. \tag{4.9}$$

The integration was started at the south pole, where $\Psi_{H,p=0}$ was arbitrarily set equal zero. The $[\overline{H_{R,p=0}}]$-data were taken from Newell *et al.* (1969) and adjusted in such a way as to end with $\Psi_{H,p=0}=0$ also at the north pole. This is not entirely justified in the extreme seasons but the surplus of net radiation balance for the total globe of either winter over summer, or vice versa, is not yet exactly known.

The energy streamfunction is shown in Figs. 9 and 10. Over the entire latitude belt 30N–90N the flux has only vertical components, in winter upward, in summer downward. In summer, the zone with almost vertically directed energy flux vector extends practically over the entire hemisphere except the innermost tropics. In the tropics there are sizeable horizontal transport components. It follows that part of the net energy flux that enters the upper surface of the atmosphere is being transported horizontally over great distances and leaves the atmosphere again without having touched the ground. In winter, some 25 units enter the upper

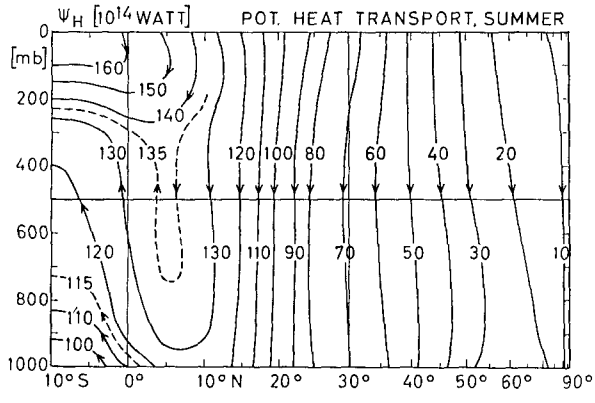

FIG. 10. Like Fig. 9 but for June–July–August.

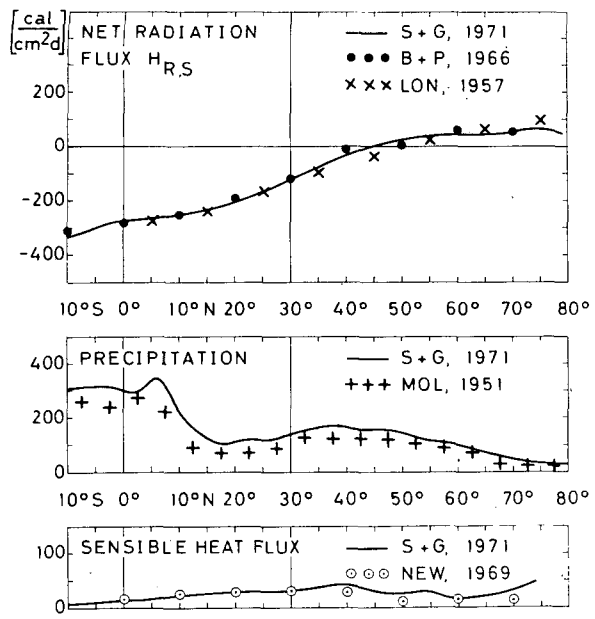

FIG. 11. Comparison of various estimates of several zonally averaged energy balance terms for December–January–February in units ly day^{-1}: $H_{R,S}$=net radiation flux at earth's surface (positive upward); precipitation (positive downward); and sensible heat flux (positive upward; note exaggerated scale). Data according to: Schutz and Gates (1971), full curves; Bernhardt and Philipps (1966), dots; London (1957), crosses; Möller (1951), plus signs; Newell *et al.* (1969), encircled dots.

atmosphere in the equatorial region, and leave it in the 30N zone. In summer, the same applies with the hemispheres reversed (isolines 130 and 160). It is obvious that the energy transports must be carried to a large degree by eddy mechanisms, since they are significantly directed against the mass transport. We like to stress this point with respect to the vertical eddy transports, which cannot be measured yet by the synoptic network. It seems very desirable to obtain reliable estimates for the vertical eddy transport components, particularly in the tropics (see Nitta and Esbensen, 1974).

One point might be noted when comparing Figs. 9 and 10 with Figs. 1 and 2: the potential heat transport is strictly in the vertical direction *outside the Hadley cells*. Horizontal components of potential heat transport are restricted to Hadley-cell latitudes. Qualitative as this pure description may appear, it should call for further physical interpretation.

In order to gain further insight into the present uncertainties of the total atmospheric energy balance, we compare various estimates of the balance terms for the season December–January–February in Fig. 11. The surface radiation flux $H_{R,S}$, according to different and independent estimates, seems to be well established. As mentioned above, the precipitation estimates are systematically different, in the tropics of the order of 80 ly day^{-1}. The sensible heat flux at the earth's surface is generally the smallest of the balance terms and of sufficient accuracy for the present purpose.

The total atmospheric energy balance in one of its many forms can be obtained by vertical integration of Eq. (4.7). Due to the various errors involved, no exact balance can be expected. We thus write for the imbalance:

$$\text{IMB}=\text{DIV}+H_{R,0}-H_{R,S}-(LP+\text{SH}). \quad (4.10)$$

We have not included the storage term explicitly because it is, on the average, only 20% of SH during the extreme seasons. The divergence term stands for:

$$\text{DIV}\equiv\frac{1}{2\pi a\cos\phi}\frac{\partial}{\partial y}(\Psi_{H,S}-\Psi_{H,0}). \quad (4.11)$$

The subscripts S, 0 denote the pressure levels surface and zero, respectively and $H_{R,0}$ and $H_{R,S}$ are the radiation fluxes across the respective pressure surfaces. It might seem daring to explicitly compare the terms in the balance equation. Newell *et al.* (1969) state that "with these uncertainties a comparison between computed atmospheric transport and observed atmospheric transport has little meaning." Despite this we have tentatively constructed meridional profiles of the 5 terms in Eq. (4.10) for northern winter. $H_{R,0}$ was taken from Newell *et al.*; $H_{R,S}$ from Schutz and Gates (1971); DIV from Fig. 9 (i.e., from Oort and Rasmusson's atmospheric data); LP+SH from Schutz and Gates (Fig. 11). The LP+SH profile was adjusted so as to give vanishing mean imbalance (correction −6 ly day^{-1}).

Fig. 12 shows that the imbalance is in general smaller in magnitude than the balance terms, although of the same order. The patterns of DIV, LP+SH, and IMB all follow the same general profile. Hence it is difficult to account for the specific errors.

The vertical energy flux across the earth's surface is partly used for driving the water flux, notably in the tropics; partly it is transported to other latitudes via oceanic currents; and partly it is stored in sensible (soil temperature increase) and latent form (variable snow and ice cover). The oceanic contribution has been estimated by Vonder Haar and Oort (1973).

5. Summary and conclusions

The general atmospheric circulation may be displayed by different methods. The set of zonally-averaged quantities is most fundamental for all studies of the global-scale circulation. The pertinent fields, if additionally averaged with respect to time, comprise category (1) of Lorenz's (1967) classification of the principal features of the circulation. It is this category with which we have been concerned in this study.

No new data in any sense have been presented. Rather, we have intended to bring together in a unified

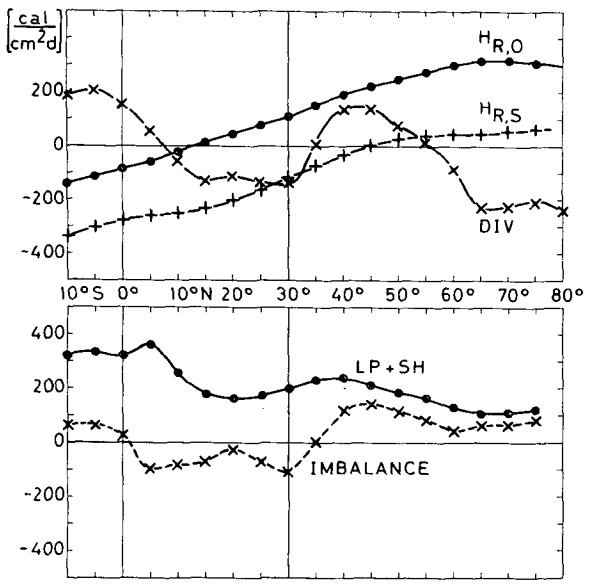

FIG. 12. Terms of zonally averaged total atmospheric energy balance equation for December–January–February in units ly day^{-1}. $H_{R,0}$, $H_{R,S}$: net radiation flux at upper and lower boundary of atmosphere, positive upward. DIV: horizontal divergence of atmospheric energy flux. P, SH: precipitation (positive downward) and surface sensible heat flux (positive upward). Imbalance according to Eq. (4.10). For data sources see text.

format and based on a comparable and consistent data set (Oort and Rasmusson, 1971) the transport patterns in the vertical-meridional plane of the relevant conservative meteorological quantities. The display in terms of a streamfunction seems to be a straightforward, though possibly not quite familiar, mode of presentation.

A synoptic view of the streamfunctions for mass, water substance, momentum, and potential heat is presented in Fig. 13 for the annual average. It is obvious that the transport vectors of different properties can cross each other and even run in opposite directions. Water and momentum transport, for instance, are directed opposite to the mean mass transport in the upper branch of the Ferrel cell. This is not surprising due to the horizontal eddy transports. But even in the Hadley cell with its high relative contribution of the mean transport, the water flux in the lower troposphere in the vicinity of the equator is in opposite direction to the mass transport. This is presumably due to vertical eddy transports caused by the hot-tower mechanism (Riehl and Malkus, 1958). In the tropics, the potential heat transport seems to parallel in a broad sense the mass transport. Between 5N and 10N, however, both transports are opposite as they are during the solstice seasons, at least in the lower troposphere. Further, the communication of moisture to the atmosphere is not quite similar to the communication of angular momentum, as stated by Newell *et al.* (1969). Rather, both fluxes are opposite over the entire region 10S–10N; similarity is only apparent over the subtropical zone 15N–30N. Several concurrent mechanisms are clearly at work which tend to blur the transport patterns.

It is important to note that the emerging mean pattern is not a mean circulation in the sense of an ideal Hadley cell. Since we have removed, notably from the momentum and energy patterns, the contribution of the mean meridional mass circulation, we have retained only relevant meteorological transport mechanisms, the contributions of the eddy exchange processes being the most significant ones. We note in passing that subtracting the mean meridional circulation from the water transport equation would have no meaning because it would introduce high fictitious reverse transports of water in the upper troposphere whereas there is no appreciable water flux at all.

The significance of the annual averaged patterns of Fig. 13 should not be overemphasized. Lorenz (1969) showed that the annual mass transport of the Hadley cell can be changed by a factor of 3 through incorporating relatively few new data. This is mainly due to the seasonal shift of the Hadley cell. During the separate seasons, the patterns are much more persistent. This might be visualized by inspecting average seasonal patterns for mean zonal wind, kinetic energy, eddy temperature, and water vapor transport for the con-

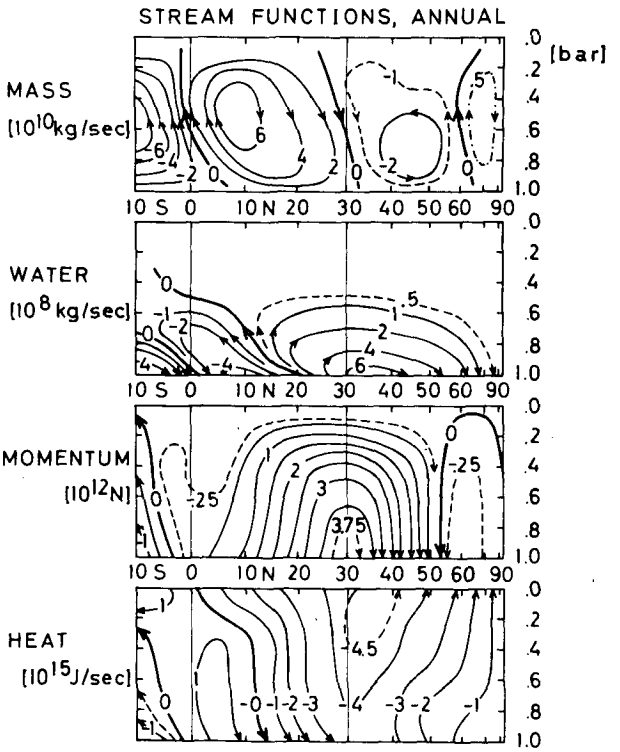

FIG. 13. Annual mean streamfunctions for atmospheric mass, water, momentum, and potential heat transport. Scaling of isolines linear except for water. Closed isolines only for mass transport which is quasi-conservative. Isolines for all other transports begin and end at horizontal boundaries of atmosphere.

secutive years 1958–1962 (Oort and Rasmusson, 1971, pp. 314–323). Although differences between the same seasons from year to year are apparent, the seasonal average of a single year is fairly representative. Changes from season to season are, on the other hand, significant.

According to Fig. 13, the various fluxes seem to be independent from each other. The interrelations are, however, important. The water flux is implicitly contained in the mass flux. In adopting this viewpoint, the mass transport streamfunction is not free of sources and sinks, either. Their effect is, however, of the order of one percent of Ψ and well below the accuracy of the data on which the Ψ-pattern is based. The heat flux pattern Ψ_H is significantly influenced by Ψ_q in the lower layers. It would have been equally possible to construct a streamfunction for the moist static energy $c_pT+gz+Lq$ instead of H (Dedenbach, 1974). The influence of the mass field on the momentum field Ψ_u has been discussed in connection with the Ω-momentum transport in Section 3. Interrelationships between momentum and energy flux field are considered by Lorenz (1969), who extensively discusses the nature of the zonally averaged circulation. In particular he maintains that not only time-averaging over one year tends to obscure many of the most interesting features of the circulation but also that zonally averaging over one latitude circle even during a specific season tends to obscure or at least distort the prevailing circulation throughout most of the tropics because of the significance of the Asiatic monsoon.

Removing the mean meridional circulation from the momentum heat transport pattern has another interesting aspect: it removes any closed streamline from the pattern. Referring back to the choice (4.5) for the mean atmospheric potential heat we note that any other specification of H_0, in particular $H_0 \equiv 0$, retains closed energy streamlines (not shown here). Similarly, Fig. 4.13 in Newell *et al.* (1972) has many closed streamlines but the removal of the back-and-forth Ω-momentum transport with aid of our Eq. (3.9) instead of (3.4) has also removed all closed streamlines. Thus a picture emerges in which the streamline pattern of a source- and sink-free quantity like mass is characterized by closed streamlines, the boundaries being also a streamline, whereas the pattern of property transports subject to sources and sinks like water, momentum, or heat has streamlines beginning and ending at a boundary. With the criterion of no closed streamlines we feel that *the streamline representation is sufficiently free of arbitrariness*. The single exception of the closed 150-isoline in Fig. 8 might be attributed to improper data handling.

The streamline representation is open to criticism. Arguments against it seem to be that several transport modes are mixed together, that irreversible source or sink terms cannot be represented by divergences of fluxes, and that zonal averages tend to severely obscure relevant meteorological processes. The first argument has already been discussed. The second can partly be considered as a matter of taste, keeping in mind Van Mieghem's (1973) terminology. Concerning the third argument the atmospheric scientist might be viewed as a photographer who tries to get 2-dimensional pictures of the 3-dimensional atmosphere. Whereas a photographer in a natural environment can use the phenomenon of perspective to good advantage in order to simulate a 3-D effect, the large-scale circulation observer has no choice but to stay within the p-y-coordinate system. It is hoped that the emerging picture still possesses enough perspective to learn a little about the nonlinear mechanisms constituting the global circulation of the atmosphere.

We finally note that the present approach is of a static rather than of a dynamic nature. The meridional transport patterns comprise the overall balance of the conservative properties but do not state anything about the forcing mechanisms of the circulation. On the other hand, the balance requirements are the necessary constraints for all possible dynamical considerations. Particularly for the design of global climate models a sound frame of consistent balance conditions is essential.

Acknowledgments. This work is part of a research project supported by the Ministry of Science and Research of the State Nordrhein-Westfalen, Germany. The author is indebted to D. Dedenbach for stimulating discussions and for the evaluation of the presented data. The calculations have been carried out on the IBM 370-165 computer of the Gesellschaft für Mathematik und Datenverarbeitung, Bonn. The figures were drawn by Miss B. Eggemann, the manuscript was typewritten by Mrs. M. Kölle. I thank the referees for suggestions which improved the quality of the paper.

REFERENCES

Augstein, E., H. Riehl, F. Ostapoff, and V. Wagner, 1973: Mass and energy transports in an undisturbed Atlantic trade-wind flow. *Mon. Wea. Rev.*, **101**, 101–111.

Bernhardt, F., and H. Philipps, 1966: Die räumliche und zeitliche Verteilung der Einstrahlung, der Ausstrahlung und der Strahlungsbilanz im Meeresniveau, Teil II und III. *Abh. Meteor. Dienst. DDR*, Nr. 77 (Bd. X), 266 pp.

Budyko, M. I., 1963: *Atlas of the Heat Balance of the Earth.* Moscow, Gidrometeoizdat., 69 pp.

Dedenbach, D., 1974: Darstellung zonal gemittelter atmosphärischer Transporte der Nordhemisphäre in Form von Stromfunktionen. Diploma Thesis, University of Bonn, May 1974, 82 pp.

Flohn, H., 1949: Eine äquatoriale Westwindzone als Glied der allgemeinen Zirkulation. *Z. Meteor.*, **3**, 240–246.

——, 1953: Wilhelm Meinardus und die Revision unserer Vorstellungen von der atmosphärischen Zirkulation. *Z. Meteor.*, **7**, 97–108.

Henning, D., 1968: Untersuchungen zur regionalen Verteilung von Transporten atmosphärischer Feldgrößen über den Äquator, Teil I: Die Verfrachtung von relativem Drehimpuls. *Beitr. Phys. Atm.* (Contr. Atmos. Phys.), **41**, 289–335.

Holland, J. Z., and E. M. Rasmusson, 1973: Measurements of the atmospheric mass, energy, and momentum budgets over a 500-kilometer square of tropical ocean. *Mon. Wea. Rev.*, **101**, 44–55.

London, J., 1957: A study of the atmospheric heat balance. Final Rept., Contract No. AF 19(122)-165, Dept. Meteor. and Oceanogr., Res. Div., College of Engineering, New York University, 99 pp.

Lorenz, E. N., 1951: Computations of the balance of angular momentum and the poleward transport of heat. Rept. No. 6, General Circulation Project, No. AF 19-122-153, 28 Feb. 1951.

——, 1967: *The Nature and Theory of the General Circulation of the Atmosphere.* Geneva, World Meteor. Organ., 161 pp.

——, 1969: The nature of the global circulation of the atmosphere: a present view. In: G. A. Corby, Ed., *The Global Circulation of the Atmosphere.* London, Roy. Meteor. Soc., pp. 3–23.

Mintz, Y., 1955: The zonal-index tendency equation. Article III in: Investigations of the General Circulation of the Atmosphere, ed. by J. Bjerknes and Y. Mintz, Final Rept., No. AF 19(122)-48. Dept. Meteor., U.C.L.A., 5 pp.

——, and N. J. Lang, 1955: A model of the mean meridional circulation. Article VI in: Investigations of the General Circulation of the Atmosphere, ed. by J. Bjerknes and Y. Mintz, Final Rept., No. AF 19(122)-48. Dept. Meteor., U.C.L.A., 10 pp.

Möller, F., 1951: Vierteljahrskarten des Niederschlags für die ganze Erde. *Peterm. Geograph. Mitt.*, **1**, 1–7.

Newell, R. E., J. W. Kidson, D. G. Vincent, and G. J. Boer, 1972: *The General Circulation of the Tropical Atmosphere*, Vol. 1. Cambridge, Mass., MIT Press, 258 pp.

——, D. G. Vincent, T. G. Dopplick, D. Ferruzza, and J. W. Kidson, 1969: The energy balance of the global atmosphere. In: G. A. Corby, Ed., *The Global Circulation of the Atmosphere.* London, Roy. Meteor. Soc., pp. 42–90.

Newton, C. W., 1971: Global angular momentum balance: Earth torques and atmospheric fluxes. *J. Atmos. Sci.*, **28**, 1329–1341.

——, 1972: Southern Hemisphere general circulation in relation to global energy in momentum balance requirements. Chapter 9 in: Meteorology of the Southern Hemisphere. *Meteor. Monogr.*, **13**, No. 35, 215–246.

Nitta, T., and S. Esbensen, 1974: Heat and moisture budget analyses using BOMEX data. *Mon. Wea. Rev.*, **102**, 17–28.

Oort, A. H., 1971: The observed annual cycle in the meridional transport of atmospheric energy. *J. Atmos. Sci.*, **28**, 325–339.

——, and E. M. Rasmusson, 1970: On the annual variation of the monthly mean meridional circulation. *Mon. Wea. Rev.*, **98**, 423–442.

——, and E. M. Rasmusson, 1971: Atmospheric Circulation Statistics. *NOAA Professional Paper 5*, U. S. Dept. of Commerce, 323 pp.

Palmén, E., and C. W. Newton, 1969: *Atmospheric Circulation Systems: Their Structure and Physical Interpretation.* New York, Academic Press, 603 pp.

——, and L. A. Vuorela, 1963: On the mean meridional circulations in the northern hemisphere during the winter season. *Quart. J. Roy. Meteor. Soc.*, **89**, 131–138.

Rasmusson, E. M., 1972: Seasonal variation of tropical humidity parameters. Ch. 5 in Newell *et al.*: *The General Circulation of the Tropical Atmosphere*, Vol. 1. Cambridge, Mass., MIT Press, 193–237.

Riehl, H., and J. S. Malkus, 1958: On the heat balance in the equatorial trough zone. *Geophysica*, **6**, 503–538.

Schutz, C., and W. L. Gates, 1971: Global climatic data for surface, 800 mb, 400 mb: January. Advanced Res. Proj. Agency Rept. No. R-915-ARPA, 173 pp.

Smagorinsky, J., 1963: General circulation experiments with the primitive equations, I. The basic experiment. *Mon. Wea. Rev.*, **91**, 99–164.

Starr, V. P., J. P. Peixoto, and R. G. McKean, 1969: Pole-to-pole moisture conditions for the IGY. *Pure Appl. Geophys.*, **75**, 300–331.

——, J. P. Peixoto, and J. E. Sims, 1970: A method for the study of the zonal kinetic energy balance in the atmosphere. *Pure Appl. Geophys.*, **80**, 346–358.

Van Mieghem, J., 1973: *Atmospheric Energetics.* Oxford, Clarendon Press, 306 pp.

Vonder Haar, T. H., and A. H. Oort, 1973: New estimate of annual poleward energy transport by Northern Hemisphere oceans. *J. Phys. Oceanogr.*, **3**, 169–172.

Vuorela, L. A., and I. Tuominen, 1964: On the mean zonal and meridional circulations and the flux of moisture in the northern hemisphere during the summer season. *Pure Appl. Geophys.*, **57**, 167–180.

White, R. M., 1949: The role of mountains in the angular-momentum balance of the atmosphere. *J. Meteor.*, **6**, 353–355.

Widger, W. K., 1949: A study of the flow of angular momentum in the atmosphere. *J. Meteor.*, **6**, 291–299.